ADVANCED FUNCTIONAL MATERIALS
www.afm-journal.de

Two are Better than One: Combining ZnO and MgF_2 Nanoparticles Reduces *Streptococcus pneumoniae* and *Staphylococcus aureus* Biofilm Formation on Cochlear Implants

Michal Natan, Fredrik Edin, Nina Perkas, Gila Yacobi, Ilana Perelshtein, Elad Segal, Alexandra Homsy, Edith Laux, Herbert Keppner, Helge Rask-Andersen, Aharon Gedanken, and Ehud Banin**

Streptococcus pneumoniae* (*S. pneumoniae*) *and Staphylococcus aureus* (*S. aureus*) are considered the most common colonizers of cochlear implants (CI), which have prompted the search for new ways to inhibit their growth and biofilm development. In the current study, CI-based platforms are prepared and sonochemically coated with ZnO or MgF_2 nanoparticles (NPs), two agents previously shown to possess antibacterial properties. Additionally, a method is developed for coating both ZnO and MgF_2 on the same platform to achieve synergistic activity against both pathogens. Each surface is characterized, and the optimal conditions for the NP homogenous distribution on the surface are determined. The ZnO-MgF_2 surface significantly reduces the *S. pneumoniae* and *S. aureus* biofilm compared with the surfaces coated with either ZnO or MgF_2, even though it contains smaller amounts of each NP type. Importantly, leaching assays show that the NPs remain anchored to the surface for at least 7 d. Finally, biocompatibility studies demonstrate that coating with low concentrations of ZnO-MgF_2 results in no toxicity toward primary human fibroblasts from the auditory canal. Taken together, these findings underscore the potential of using NP combinations such as the one presented here to efficiently inhibit bacterial colonization and growth on medical devices such as CIs.

1. Introduction

Over the past 30 years, Cochlear implants (CIs) have become the gold standard for treating profound hearing loss.[1] However, there are potential infectious complications of CIs, including postoperative wound and device-related infections as well as bacterial meningitis.[2] In particular, children who have a CI may experience acute otitis media that can lead to inner-ear infections, device infections, device extrusion or failure, and/or meningitis. Many of the CI-associated infections result from biofilm formation on the implant. Bacteria tend to colonize and adhere to abiotic surfaces as well as to biotic ones and form structured communities called biofilms, which are held together by an extracellular matrix that consists mainly of proteins and exopolysaccharides.[3,4] Biofilm formation plays a critical role in most device-related infections. Biofilms are extremely difficult to eradicate due to their increased antibiotic resistance and efficient ability to evade the host immune system, which hinders treatment and ultimately culminates in prolonged hospitalization periods and patient mortality.[5–7]

Streptococcus pneumoniae (*S. pneumoniae*) and *Staphylococcus aureus* (*S. aureus*) are gram-positive bacteria that typically colonize the respiratory tract, sinuses, and nasal cavity and, in some cases, spread to other parts of the body. *S. pneumoniae* and *S. aureus* are the most common pathogen causing CI-associated infections.[1–3,8] Therefore, there is an urgent need to find innovative and creative solutions to inhibit their growth and

M. Natan, G. Yacobi, Prof. E. Banin
The Mina and Everard Goodman Faculty of Life Sciences
and the Center for Advanced Materials and Nanotechnology
Bar Ilan University
Ramat Gan 52900, Israel
E-mail: ehud.banin@biu.ac.il
F. Edin, Prof. H. Rask-Andersen
Department of Surgical Sciences
Section of Otolaryngology
Uppsala University Hospital
SE-751 85, Uppsala, Sweden
Prof. N. Perkas, Dr. I. Perelshtein, E. Segal, Prof. A. Gedanken
Department of Chemistry and the Center
for Advanced Materials and Nanotechnology
Bar-Ilan University
Ramat Gan 52900, Israel
E-mail: aharon.gedanken@biu.ac.il
Dr. A. Homsy, Dr. E. Laux, Prof. H. Keppner
Haute Ecole Arc Ingénierie
HES-SO//University of Applied Sciences Western Switzerland
Eplatures-Grise 17, CH-2300 La Chaux-de-Fonds, Switzerland

DOI: 10.1002/adfm.201504525

biofilm formation on CIs. In the last several years, the application of inorganic nanoparticles on medical implants has been found to represent a promising strategy to minimize medical implant associated infections.[5–7,9] For example, several studies have demonstrated that silver NPs have enhanced antimicrobial activity compared to silver ions.[10,11] Other metals, such as gold, have also been shown to have strong antimicrobial activities against a wide range of pathogenic microorganisms.[12] Further, nanoscaled zinc oxide ZnO was demonstrated to be an effective reagent against various types of bacterial infections and against biofilms including *S. pneumoniae*.[13–19]

Our previous studies have demonstrated that ultrasound assisted deposition is a simple and robust technique for achieving uniform distribution and strong anchoring of NPs onto various substrates.[20,21] Using this method, ZnO NPs sonochemically deposited on glass surfaces were shown to significantly inhibit biofilm growth of the gram-negative bacteria *Escherichia. coli* (*E. coli*) and inhibit to a lesser extent the growth of the gram-positive bacteria *S. aureus*.[22] Using similar sonochemical coating methods, the antimicrobial activity of a different kind of NP, MgF_2, has also been investigated.[23,24] Urine catheters coated with MgF_2 NPs using sonochemistry were shown to provide long-lasting self-sterilizing properties. Notably, the MgF_2 coating showed an opposite trend to ZnO NPs in that biofilm development of *S. aureus* was significantly attenuated while that of *E. coli* was only mildly affected.[23]

The antibiofilm properties of sonochemically prepared ZnO and MgF_2 NPs against *S. pneumoniae*, the upper respiratory track pathogen commonly associated with CI implant infections, have not been studied to date. Based on previous results, we hypothesized that a surface nanofabricated with both ZnO and MgF_2 may exhibit the combined antibiofilm properties of both agents, thus counteracting the adherence capability of *S. pneumoniae*. Additionally, *S. aureus,* which causes the majority of CI wound infections, might be affected by a surface combining both ZnO and MgF_2 NPs. Accordingly, the aim of the present work was to identify the optimal coating that will prevent the formation of both *S. pneumoniae* and *S. aureus* biofilms on a CI-based platform using ZnO and MgF_2 NPs and/or a combination of these two materials. The coating procedure was performed via the in situ sonochemical method using zinc and magnesium acetates as the precursors. The surfaces for deposition were silicone prototypes of CI electrodes, which were manufactured by MED-EL Company (Austria). Our results demonstrate that combining both ZnO and MgF_2 on a single surface indeed provides synergistic antibiofilm activity against *S. pneumoniae* and *S. aureus* compared to surfaces coated with only ZnO or MgF_2 nanostructures. Furthermore, biocompatibility studies performed with primary human dermal fibroblasts (HF) isolated from the auditory canal indicate no acute toxicity of the ZnO-MgF_2 NP coating.

2. Results and Discussion

2.1. Structure and Morphology of the Coated Surfaces

The CI-based platforms were created by coating a silicone substrate with a Parylene film, which confers low water permeability and enhanced biocompatibility.[25] Silicone used alone as a layer on the implant provides biocompatibility but allows water penetration; the latter may affect the electrical properties of the device such as the impedance. Adding a Parylene layer on the CI, although not a typical procedure, blocks water permeability into the device and can improve its functionality.[25] Henceforth, "CI" will refer to the Parylene-silicone CI-based platform, and "coating" will refer to the NPs. The sonochemical deposition was carried out by ultrasound-assisted irradiation of the precursor solution in the presence of the solid surface; this coating procedure is called in situ. In this process, microjets that form after the collapse of acoustic bubbles throw the just-formed NPs at the surface of the substrate at such high speeds that they strongly adhere to the solid surface and even penetrate it.[21,26] In the case of ZnO NPs, the sonication of zinc acetate with the addition of ammonia in a water–ethanol solution results in the formation and simultaneous deposition of ZnO NPs on the Parylene layer of the silicone surface. Similarly, the MgF_2 NPs were formed by interaction of magnesium acetate and hydrofluoric acid in ethanol solution and were deposited on the Parylene layer by the above-mentioned microjets.

The structure and composition of the deposited materials were evaluated by X-ray diffraction (XRD). The XRD patterns of ZnO NPs sonochemically deposited on the CI surface reveal that ZnO NPs are crystalline in nature (Figure SI-1, Supporting Information). The main diffraction peaks at $2\theta = 31.77°$, 34.42°, and 36.25° can be assigned to the (100), (002), (101) planes of ZnO. These diffraction lines correspond to the hexagonal phase of ZnO (PDF: 89–7102).

The XRD patterns of MgF_2 NPs are presented in Figure SI-2 (Supporting Information). The reflection peaks at $2\theta = 27.21°$, 40.40°, 53.62°, and 68.01° correspond to the crystalline planes (110), (111), (211), and (301) of tetragonal MgF_2 (PDF 41–1443). The diffraction patterns are highly broadened because of the small dimension of the particles. According to the Debye–Scherer calculation, the crystallite size of the MgF_2 NPs is 25 ± 5 nm. Of note, this calculation could not be done for the ZnO NPs because it is only suitable for particles smaller than 0.1 μm.

The morphology of ZnO NPs deposited on the CI surface was examined by scanning electron microscopy (SEM) (**Figure 1**). The SEM image shows that the coating is homogeneous and that the particles are uniform in size (Figure 1a), with an average particle size of 200 ± 30 nm (Figure 1b). The concentration of ZnO NPs deposited on the surface was determined by inductively coupled plasma (ICP) analysis and found to be 0.3 ± 0.03 wt%.

Because the sonochemically synthesized MgF_2 NPs are very small, they could only be visualized properly by high-resolution SEM (HRSEM) (**Figure 2**). As demonstrated in Figure 2a, uniform coating of MgF_2 NPs on the CI surface was achieved with an average particles size of 25 ± 5 nm (Figure 2b), which agrees well with the XRD results (Figure SI-2, Supporting Information). The concentration of the MgF_2 NPs deposited on the surface as determined by ICP was 0.22 ± 0.03 wt%.

Two different approaches were applied for the co-deposition of ZnO and MgF_2 NPs on the CI surface. The first was the "throwing stones" (TS) method developed for the deposition

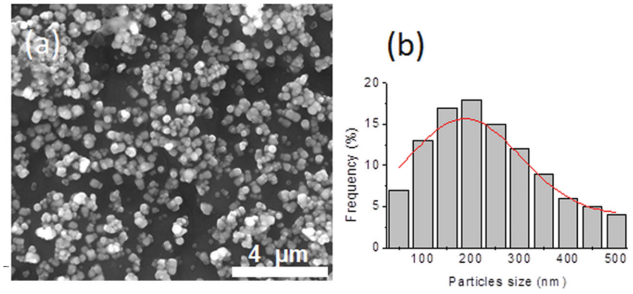

Figure 1. SEM analysis of ZnO NPs deposited on the CI surface: a) SEM image (magnification: 20 000×); b) size distribution histogram of the ZnO NPs. A SEM image of an uncoated Parylene-silicone surface is provided in Figure SI-3 (Supporting Information).

of commercially available NPs or for anchoring prefabricated NPs.[27] In this method, already synthesized nanoparticles are added to the solution and thrown at the solid surface by ultrasound-assisted irradiation of the solution. The second method is based on stepwise sonochemical deposition, whereby one of the materials is deposited in situ by sonochemical irradiation of the corresponding precursor, and the second layer is then anchored by the "throwing stones" method. Optimization of the co-deposition processes is summarized in **Table 1**. The initial molar ratio of the precursors was chosen to be 1:1. The morphology of the coated CI surface was analyzed by SEM (**Figure 3**), and the concentration of the deposited materials was determined by ICP.

The concentration of MgF_2 NPs on CI surfaces prepared by simultaneous deposition using the TS mode was 0.08 wt%, while that of ZnO was only 0.03 wt% (sample A). When the MgF_2 NPs were deposited as the first layer by the in situ mode and the second layer of ZnO NPs by the TS mode (sample B), the MgF_2 content increased to 0.14 wt%, but the ZnO content was still very poor (0.02 wt%). In agreement with the ICP analysis, the SEM analysis showed that the depositions in the cases of samples A and B were not optimal as only a limited amount of NPs with sizes between 300 and 650 nm were observed (Figure 3a,b). Our interpretation is that the difference in particle size of MgF_2 and ZnO underlie these observations. The small MgF_2 NPs are thrown at the surface at higher speeds and are therefore embedded better in the surface of the substrate. By contrast, the ZnO NPs are larger in size and tend to aggregate in the liquid according to the Ostwald ripening

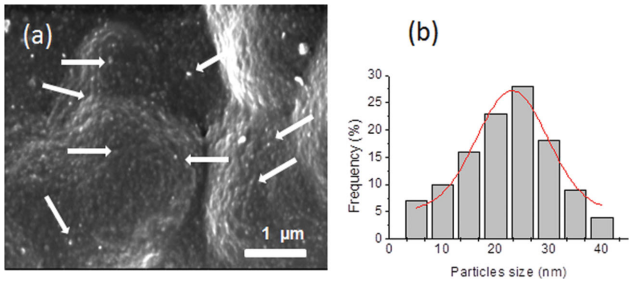

Figure 2. HRSEM analysis of MgF_2 NPs deposited on the CI surface: a) HRSEM image (magnification: 50 000×); b) size distribution histogram of the MgF_2 NPs. Some MgF_2 NPs are indicated with arrows.

Table 1. Optimization of the co-deposition process for combining ZnO and MgF_2 NPs on the Parylene-silicone surface.

Samples	Co-deposition approach	Particle size [nm]	Concentration of coated material [wt%]
A	Simultaneous deposition with ZnO and MgF_2 in (TS) mode	350–650	ZnO – 0.03 ± 0.005
			MgF_2 – 0.08 ± 0.005
			Σ = 0.011 ± 0.01
B	Stepwise deposition:	300–400	ZnO – 0.02 ± 0.005
	1 – MgF_2 in situ		MgF_2 – 0.14 ± 0.005
	2 – ZnO by TS		Σ = 0.016 ± 0.01
C	Stepwise deposition:	200–300	ZnO – 0.16 ± 0.03
	1 – ZnO in situ		MgF_2 – 0.13 ± 0.03
	2 – MgF_2 by TS		Σ = 0.29 ± 0.06
D	ZnO in situ with MgF_2 added during reaction	300–500	ZnO – 0.17 ± 0.03
			MgF_2 – 0.13 ± 0.03
			Σ = 0.30 ± 0.06

mechanism. Thus, they do not impact the surface at the same speed, resulting in insufficient adherence to the surface.

This difficulty can be overcome by depositing ZnO NPs via the in situ method in the first stage. Using this approach, very small seed particles are deposited on the surface, which can continue to grow as previously observed in the deposition of silver NPs.[26] Indeed, the highest percentage of both components (0.3 wt%) and the most uniform distribution of NPs on the CI surface were achieved when the ZnO NPs were coated using the in situ sonication procedure, and the previously synthesized MgF_2 NPs were deposited as a second layer via the TS method (sample C, Figure 3c). This co-deposition approach takes advantage of the strong adhesion of ZnO NPs to the surface, which are not removed even when sonication is repeated during

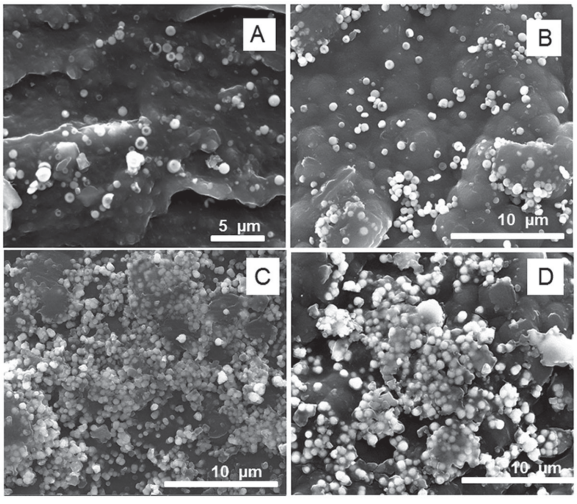

Figure 3. SEM images of mixed ZnO-MgF_2 sonochemical deposition. a–d) Each panel is labeled according to the co-deposition approaches described in Table 1 (magnification: 10 000×).

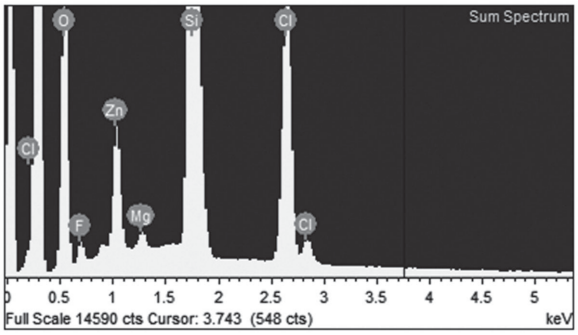

Figure 4. EDX analysis of ZnO-MgF_2 sonochemical deposition on the CI (sample C).

deposition of the prefabricated MgF_2 NPs. In sample D, when the MgF_2 NPs were added as "throwing stones" to the working solution during in situ deposition of ZnO (i.e., the coating of both NPs was performed simultaneously), the percentage of components on the surface was similar to that obtained when preparing sample C. However, the distribution of NPs on the surface was less homogeneous (Figure 3d) than in the case of the stepwise deposition (Figure 3c). Based on these findings, the co-deposition approach used in the preparation of sample C was deemed optimal, and CI surfaces prepared in this way were further characterized using energy dispersive X-ray (EDX). The EDX analysis clearly demonstrates the presence of both phases of ZnO and MgF_2 on the coated surface (**Figure 4**).

To minimize the possibility that the coated CI would be toxic to neuron cells, we further reduced the levels of the components on the surface achieving a final level of 0.06 wt% ZnO and 0.02 wt% MgF_2, reaching a total of 0.08 wt%. The co-deposition on the CI was carried out in the same manner as described for sample C. The low concentration was achieved by reducing the concentration of the zinc acetate precursor from 0.01 to 0.005 mol L^{-1} and the sonication time from 30 to 10 min. A homogeneous coating of ZnO and MgF_2 NPs was observed on the CI surface by SEM (**Figure 5**a,b). A selected area in an HRSEM image was analyzed using elemental dot mapping (Figure 5c). The contents of zinc, oxygen, magnesium and fluorine in the mapped area are represented in parts d, e, f, and g of Figure 4, respectively.

Table 2. Release of ions into the leaching solution after 24 h.

	Concentration of ions in leaching solution ($\times 10^{-5}$ mol L^{-1})		
	Saline		Perilymph
Coating material	Zn^{2+}	Mg^{2+}	Zn^{2+}
ZnO 0.3 wt%	3.9 ± 0.4	–	7.7 ± 0.8
MgF_2 0.2 wt%	–	3.2 ± 0.3	–
ZnO (0.17 wt%) MgF_2 (0.13 wt%)	1.4 ± 0.15	0.9 ± 0.1	3.1 ± 0.3

2.2. Leaching Studies of the Sonochemically Coated Substrates

The durability of the NP deposition was investigated using a leaching test. We carried out leaching experiments in two media: a saline solution and a perilymph solution (the extracellular fluid located within the cochlea). We studied the leaching of NPs and ions. The release of ions from the surface into the solution after 24 h was measured by ICP, and the results are presented in **Table 2**. The partial release of Zn^{2+} and Mg^{2+} ions from the surface to the surrounding liquid corresponds to the equilibrium solubility constants of ZnO and MgF_2 in water, i.e., (K_{sp}ZnO = 10^{-10}–10^{-11}) and ($K_{sp}MgF_2$ = 10^{-9}–10^{-10}).These data indicate that the release of Zn^{2+} and Mg^{2+} ions from the ZnO-MgF_2 coating into saline solution is 2.8 and 3.5 times less than that released when ZnO or MgF_2 are deposited separately, respectively. It is important to note that the leaching of Mg^{2+} into the perilymph cannot be determined because of the high initial concentration of Mg^{2+} in this medium; therefore, the leaching of the ZnO-MgF_2 coating into the perilymph can be evaluated based only on measurements of Zn^{2+}. The release of Zn^{2+} ions into the perilymph solution is two times higher than that observed for the saline solution. The higher solubility of ZnO in perilymph can be explained by the presence of organic compounds, which most likely affect the K_{sp} of ZnO. It is also possible that the ionic strength of the perilymph solution is a determining factor in the dissolution of ZnO. Nevertheless, the release of Zn^{2+} ions from the ZnO-MgF_2 coating in perilymph is 2.5 times lower than that observed for the ZnO coating alone. Of note, similar leaching results were obtained after 7 d of exposure to either saline or perilymph (Table SI-1, Supporting Information) Taken together, these results suggest that there is a further advantage to using the ZnO-MgF_2 coating over the deposition of individual NPs, as the stability of the coating is increased.

Additional leaching experiments were conducted to monitor the release of NPs from surfaces coated with either ZnO or MgF_2 or the combination of both materials. The first

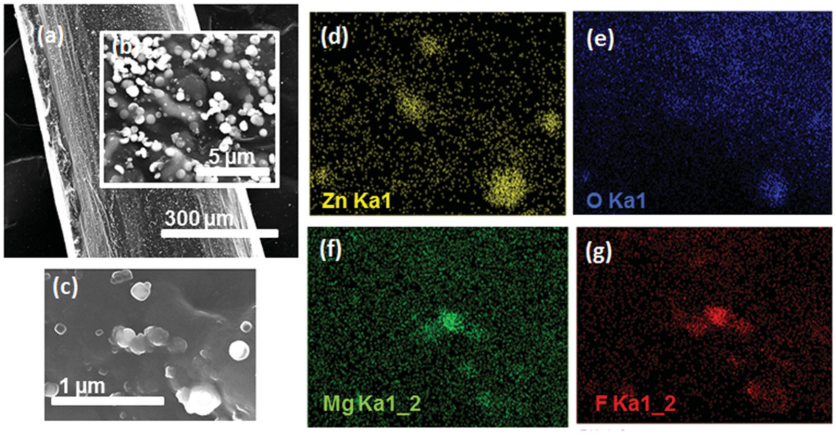

Figure 5. HRSEM analysis of ZnO-MgF_2 sonochemical deposition on the CI surface: a) image of the CI coated with ZnO-MgF_2 NPs (magnification: 300×); b) the inset image is taken at a higher magnification (20 000×); c) selected image for X-ray dot mapping (magnification: 50 000×); X-ray dot mapping for d) zinc, e) oxygen, f) magnesium, and g) fluorine.

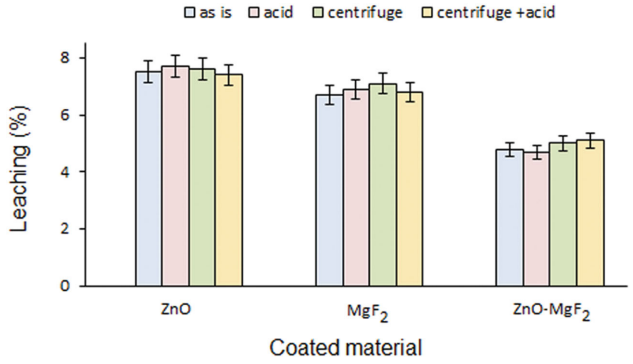

Figure 6. ICP analysis of leaching under various experimental conditions after 24 h of exposure to a saline solution. The data showing the ion concentrations are provided in Table SI-2 (Supporting Information).

two methods used to monitor NP leaching were dynamic light scattering (DLS) and transmission electron microscopy (TEM); NPs were not detected in the leaching solution using either technique (data not shown). We utilized ICP to further corroborate these results. The ion concentrations after 24 h of leaching were compared with those obtained after the addition of HNO_3. We reasoned that, if there were NPs from the coating in the leaching solution, the HNO_3 would dissolve the NPs, and the concentrations would increase. **Figure 6** shows that the ion concentrations before and after the HNO_3 addition are identical. These results further indicate no leaching of the NPs into the saline solutions. In fact, four different ICP modes were applied: (i) after incubation of the surface with the solution (as described above), (ii) after addition of HNO_3 to the probe solution, (iii) after the washing solution was centrifuged (16000 rpm) using a Millipore ultrafiltration tube filter 3000 Molecular Weight Cut-Off (MWCO), and (iv) the same as (iii) after addition of HNO_3 to the filtrate. HNO_3 was added to ensure any leached NPs would be dissolved, with the expectation that this would result in an increase in the amount of Zn^{+2} ions detected by ICP (serving as "positive" controls in the case that NPs were released). Conversely, the centrifugation step was conducted with the expectation that some NPs would be removed, resulting in a decrease in the amount of Zn^{+2} ions detected by ICP analysis (serving as "negative" controls in the case that NPs were released). No differences were found between the Zn^{2+} and Mg^{2+} ion concentrations after the addition of acid to the surfaces and with and without centrifugation, corroborating the hypothesis that no NPs leached from the surface under the applied conditions (Figure 6).

Taken together, the ICP results indicate that there is no release of NPs into the washing solution, which means that ions are partially dissolved in the aqueous media, but no particles are dissolved. Thus, both the ZnO and MgF_2 NPs are strongly adhered to the CI surface. Moreover, according to the SEM results, the majority if not all of the NPs remained deposited on the surface after the leaching procedure (**Figure 7**).

2.3. Antibiofilm Activity

Next, the potential of either ZnO or MgF_2 sonochemically deposited NPs to reduce biofilm formation of *S. pneumoniae*

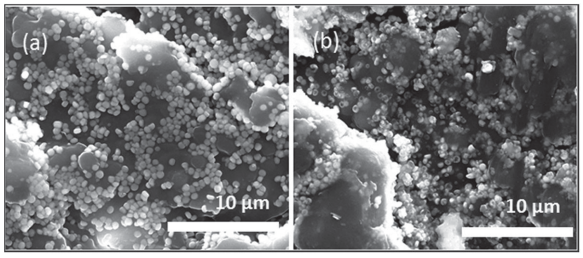

Figure 7. SEM analysis of ZnO-MgF_2 sonochemical deposition on the CI surface: a) as prepared, b) after 7 d of leaching in saline (magnification: 10 000×).

and *S. aureus* was evaluated. CI surfaces coated with ZnO NPs reduced biofilm development of *S. pneumoniae* by slightly more than 1 log and compromised the biofilm viability of *S. aureus* by 4 logs; however, surfaces coated with MgF_2 NPs slightly reduced the biofilm of either of the bacteria (**Figure 8**). Notably, CI surfaces coated with both ZnO and MgF_2 NPs compromised the biofilm growth by more than 2 logs and 6 logs for *S. pneumoniae* and *S. aureus*, respectively, even though the concentration of each NP type was almost half that found on surfaces coated with either ZnO or MgF_2 (Table 1 and ICP results presented in section 3.1). This finding indicates that the combination of both NPs on a single surface results in a synergistic activity against *S. pneumoniae* and *S. aureus* biofilm growth. It is worth noting that, even when the NPs were deposited at a

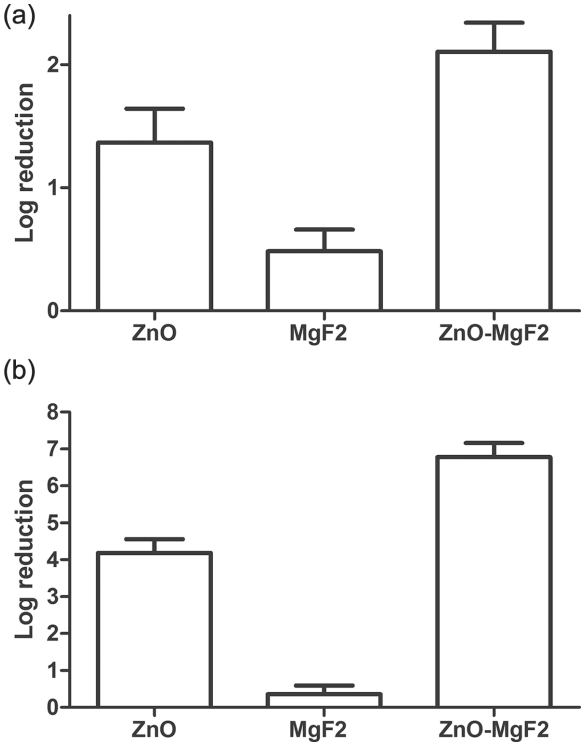

Figure 8. Synergistic antibiofilm activity of ZnO-MgF_2-coated CI surfaces. CIs coated with either ZnO or MgF_2 NPs or the combination of both materials were exposed to a) *S. pneumoniae* or b) *S. aureus* as described in the methods section, and the biofilm growth was determined using viable counts. The data shown represent the average of at least three independent experiments.

fourth or at a tenth of the initial concentration, the surface with both NPs was still active against *S. pneumoniae* and *S. aureus* biofilms, respectively (Figures SI-4 and SI-5, Supporting Information). Silver is one of the most bactericidal agents, making it a good candidate for coatings.[28] Indeed, silver NPs deposited on catheters reduced the biofilm of *S. aureus* by 93%,[29] suggesting that our results are quite dramatic and significant because the ZnO-MgF_2 prototype managed to reduce the biofilm by 99.9% (Figure 8b). Furthermore, the exceptionally reported slippery liquid-infused porous surface demonstrated a similar reduction of 97.2% for *S. aureus,* corresponding to a reduction of 1–2 orders of magnitude.[30]

2.4. Biocompatibility

Finally, we examined the biocompatibility of the ZnO-MgF_2-coated CI. Cultured primary human fibroblasts isolated from the auditory canal were incubated with fragments of coated and uncoated CIs. The impact on cell viability was measured using the alamarBlue fluorescent substrate, and the fluorescence was measured at 24 and 48 h. A higher signal means higher cell metabolism and viability in the well, which indicates better biocompatibility of the material. There was a 20% reduction in alamarBlue signal from HF cultured with uncoated CI fragments relative to the HF cultured in an empty microplate well (without any fragment in place). This could be explained by some adverse effects on cell viability from the Parylene layer (generally considered inert and biocompatible)[25] and/or a mechanical effect of the free-floating implant fragments. Alternatively, as the readings were performed with the fragment inside the wells, this phenomenon could also be an effect of shadowing. In this regard, because all the CI fragments were cut to the same size, any shadowing effect should be equal for all the samples. Nevertheless, when determining the biocompatibility of ZnO-MgF_2-coated CI, the values were normalized against the value for uncoated CI ("Parylene") (**Figure 9**).

There was a significant decrease in cell viability caused by the CI coated with 0.32 wt% ZnO-MgF_2 at both 24 h (Kruskal Wallis test $p = 0.0003$) and 48 h ($p < 0.0001$). By contrast, the viability of cells exposed to the CI coated with 0.08 wt% ZnO-MgF_2 was comparable to uncoated CI at the 24 h time point, with only a non-significant difference observed at 48 h. This finding suggests that the NPs have a minor but concentration-dependent impact on cell health, which is promising when considering future clinical applications of CIs coated with low concentrations of ZnO-MgF_2.

In addition, the biocompatibility of the 0.08 wt% ZnO-MgF_2 CI was evaluated using mouse 3D cultured neurons (**Figure 10**). Mouse modiolus explants containing spiral ganglion neurons were placed in close proximity to the coated and uncoated CIs and cultured for 8 d, as described in the materials and methods section, before the growth of neural extensions was monitored by staining for the neural marker β-III tubulin (Tuj1).

Outgrowth from explants is dependent on the way the modiolus is cut and where the ganglion is located within the sample and is therefore highly variable. This behavior makes it difficult to analyze whether the outgrowth direction is affected by the material, particularly when the sample size is small.

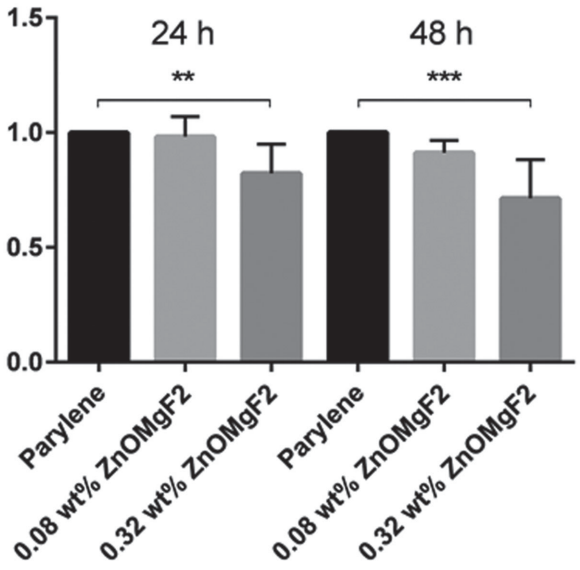

Figure 9. Biocompatibility study using primary human fibroblasts. Mean values of alamarBlue signals normalized against Parylene at 24 and 48 h. HF were cultured together with uncoated or ZnO-MgF_2 (0.08/0.32 wt%)-coated CI fragments in culture media supplemented with 10% alamarBlue. The results show the average of six independent experiments. The higher the concentration of the coating, the greater the inhibition of HF growth, indicating a concentration dependent effect. (**$p = 0.0003$, ***$p < 0.0001$).

Nevertheless, we observed that neurons sprouted in all gels, regardless of which material was in the gel, suggesting that the presence of the CI fragments had no acute toxic effects during the 8 d culture period. This interpretation is further supported by laser confocal microscopy analysis, which showed that neurons reached the CI coated with ZnO-MgF_2 and interacted with the silicone surface (Figure 10d) where they grew underneath and along the ZnO-MgF_2-coated surface. Because the functionality of the CI in patients relies on functional spiral ganglion neurons, this preliminary finding that cultured neurons can re-sprout neurites that interact with the ZnO-MgF_2-coated surface is encouraging, as it suggests that spiral ganglions can withstand any leaching from the NP coatings.

3. Conclusions

In the present study, we examined the impact of sonochemically coating CIs with ZnO, MgF_2, or ZnO-MgF_2 NPs on biofilm formation by *S. pneumoniae* and *S. aureus*. SEM analysis of CI-based platforms showed that ZnO and MgF_2 are uniformly deposited on the surface with average sizes of 200–300 nm and 25 nm, respectively. In this study, we aimed at combining both types of NPs on the same surface to enhance their antibiofilm activities. The most uniform distribution of a combination of ZnO and MgF_2 NPs on the CI-based platform was achieved when ZnO was first coated by the in situ method, and then, MgF_2 NPs were embedded by the TS method. Importantly, the combination of ZnO and MgF_2 on a single surface was found to display synergistic activity against *S. pneumoniae* and *S. aureus* biofilm development. Leaching experiments indicated that the

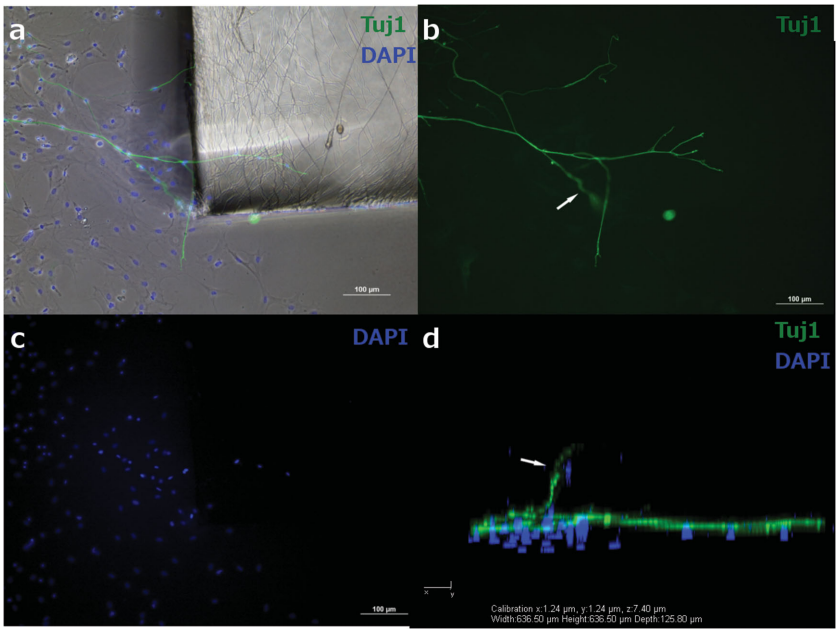

Figure 10. Biocompatibility with 3D cultured neurons. Mouse modiolus explants containing spiral ganglion neurons were placed in close proximity to CI coated with 0.08 wt% ZnO-MgF_2 and cultured for 8 d, as described in the Experimental Section, before staining against neural marker β-III tubulin (Tuj1) to monitor neurite outgrowth. a) Merged image of phase contrast and fluorescent images with Tuj1 positive (green) neurites growing toward and underneath the coated CI surrounded by DAPI-stained nuclei (blue). b,c) Blue and green channels of (a) shown separately. d) Confocal Z-stack of the same region as shown in (a)–(c) tilted so that the out of focus neuron from B (arrow) becomes visible (arrow).

mixed coating is stable for at least a week, demonstrating that the sonochemical method results in strong adhesion of ZnO-MgF_2 NPs. To further investigate the potential toxicity of a ZnO-MgF_2 surface, we examined its impact on the viability of primary human dermal fibroblasts isolated from the auditory canal. CI fragments coated with a low concentration of ZnO-MgF_2 did not exert noticeable adverse effects, underscoring the advantage of using this NP combination. Taken together, the results of this study demonstrate the potential of using NP combinations to achieve synergistic antibiofilm activity in various medical applications.

4. Experimental Section

Coating Procedure: All chemicals were purchased from Sigma-Aldrich Company and used without further purification. The CI-based platforms were created by coating a silicone substrate with a Parylene film, which confers low water permeability and biocompatibility.[25] The Parylene film had an average thickness of 1.2 µm and was created at the HES-SO University of Applied Sciences (Switzerland). Henceforth, "CI" will refer to the Parylene-silicone CI-based platform and "coating" will refer to the NPs.

The ZnO NPs were deposited on a CI electrode via the sonochemical irradiation of $Zn(Ac)_2.2H_2O$ in a water–ethanol solution (volume ratio 1:9). The concentration of the precursor varied across the range 0.005–0.02 mol L^{-1} Zn^{2+}. The pH of the reaction slurry was adjusted to 8 via the addition of a 25% ammonia solution. The CI electrode was inserted into the reaction vessel, and the sonication was performed by immersing a Ti-horn (20 kHz, 600 W at 30% efficiency; Sonics and Materials, Newton, CT) for various periods of time. After the reaction, the NP-coated electrode was washed with water and ethanol and allowed to dry in air at room temperature. It is known that the antimicrobial activity of ZnO NPs depends on their size, where reducing the particle size enhances antimicrobial activity.[31] To achieve the most uniform distribution of ZnO NPs on the substrate, the coating conditions were optimized by changing the reagent concentration, reaction temperature, duration of coating, and addition of a capping agent (PVP). As a result, the following parameters were chosen for the optimal deposition procedure: concentration of Zn^{2+} 0.01 mol L^{-1}, concentration of PVP 0.3 g L^{-1}, reaction temperature 20 °C, and sonication time 30 min. The MgF_2 NPs were deposited on the CI electrode by sonochemical irradiation of 0.02 M $Mg(Ac)_2.4H_2O$ in ethanol with the addition of 0.01 M HF (1:2 equivalent ratio). The mixture was irradiated with Ti-horn at 20 °C for 30 min. The hybrid ZnO-MgF_2 was prepared as follows: First, MgF_2 NPs were prepared by sonication of 0.02 M $Mg(Ac)_2$.4H2O in ethanol with the addition of 0.01 M HF (1:2 equivalent ratio). The slurry was irradiated with a Ti-horn at 20 °C for 30 min. The precipitate was separated by centrifugation, washed with ethanol, and dried under vacuum. The ZnO NPs were deposited on a CI electrode by the sonochemical irradiation of $Zn(Ac)_2.2H_2O$ in a water–ethanol solution (volume ratio 1:9). The concentration of the precursor varied in the range 0.005–0.02 mol L^{-1} Zn^{2+}. Then, 0.3 g L^{-1} PVP was added to the reaction slurry to prevent increases in the particles size. The pH of the reaction slurry was adjusted to 8 via the addition of a 25% ammonia solution. The CI electrode was inserted into the reaction vessel, and the sonication was performed by immersing a Ti-horn (20 kHz, 600 W at 30% efficiency; Sonics and Materials, Newton, CT) for 30 min. After the reaction, the ZnO-coated electrode was washed with water and ethanol and allowed to dry in air at room temperature. For the deposition of the MgF_2 layer on the ZnO-coated electrode, 0.1 g MgF_2 powder was dispersed in 50 mL of ethanol, and the CI electrode coated with ZnO was inserted into the reaction vessel. Then, the sonication was performed by immersing a Ti-horn (20 kHz, 600 W at 30% efficiency) for 15 min. After the reaction, the electrode coated with ZnO-MgF_2 NPs was washed with ethanol and allowed to dry in air at room temperature.

Physical-Chemical Characterization: The crystallinity of the NPs was verified by XRD using a D8 Bruker Company diffractometer using Cu Kα 1.541 Å radiation. The morphology of the coating was characterized by SEM on a Quanta 200F FEG 250 scanning microscope (FEI) and HR-SEM was carried out on a Magellan 400L microscope (FEI). The amount of NP material deposited on the electrode was determined by boiling the coated electrode in 5 M HNO_3 to dissolve the ZnO and the MgF_2 followed by quantification using inductive coupled plasma-atomic emission spectroscopy on an ICP-spectrometer ULTIMA 2501 JOBIN-YVON (Horiba). In parallel, the content of the coated material on the surface was also measured using the EDX method.

Leaching of the deposited material was tested in saline solution (0.9% NaCl) as well as in artificial perilymph. The artificial perilymph was prepared by the following protocol: 145.5×10^{-3} M NaCl, 2.7×10^{-3} M KCl, 2.0×10^{-3} M MgSO4, 1.2×10^{-3} M $CaCl_2$, and 5.0×10^{-3} M HEPES (4-(2-hydroxyethyl)-1-piperazineethanesulfonic acid) were dissolved in double-distilled water, and the pH was adjusted to 7.4 with NaOH. The leaching was monitored by placing the coated sample (0.1 g) in 5 mL of probe solution and incubating at 37 °C with shaking at 100 rpm. The washing solution was replaced every 24 h for 7 d and analyzed by ICP for the presence of ions. After the leaching procedure was terminated, the coating was analyzed by SEM. The release of NPs into the liquid

(saline or perilymph) was determined by DLS of a sample of the leached solution using the Malvern Zetasizer Nanoseries Instrument and by TEM (JEOL Jem-1400 120 kV). In addition, to follow the leaching of NPs into the above-mentioned solutions, the ICP analysis was repeated at four different stages: (i) as prepared, (ii) after the addition of HNO_3, (iii) after centrifugation (16 000 rpm) with Millipore ultrafiltration tube filter 3000 MWCO, and (iv) with the addition of HNO_3 to the filtrate.

Antibiofilm Activity against S. pneumoniae and S. aureus: The antibiofilm activity of the coated CIs (1 cm × 1 cm) was determined using the static biofilm formation assay. *S. pneumoniae* (clinical isolate) was streaked on a blood agar plate (Hylabs), which was incubated at 37 °C under a low oxygen environment (Oxoid AnaeroGen Sachet, Thermo Scientific). *S. aureus* FRF1169 was grown overnight at 37 °C under agitation (250 rpm) in Tryptic Soy Broth (TSB, Difco). On the following day, *S. pneumoniae* was transferred from the solid blood agar plate to a 15 mL tube filled with Brain Heart (BH, Difco) medium supplemented with 1% Glucose (BH-Glu) and grown at 37 °C under agitation (250 rpm) for 6–8 h. Then, working solutions with an OD595 of 0.3 or 0.01 (corresponding to approximately 3×10^8 and 10^7 colony-forming units/mL) for *S. pneumoniae* and *S. aureus,* respectively, were prepared using Muller Hinton medium (MH, Difco) supplemented with 1% (*S. pneumoniae*) or 0.2% (*S. aureus*) Glucose (MH-Glu). Next, 2.8 mL (*S. pneumoniae*) or 1 mL (*S. aureus*) of the working solutions were placed into each well in a 24-well plate (DE-GROOT) that contained each of the CI fragment samples glued to the bottom of the well, such that the coated side was facing the bacterial solution. The plates were then wrapped with a wet paper and a bag to provide a humid environment and incubated at 37 °C for 18–20 h. Following overnight incubation, the biofilms were stripped from the CI fragment samples as follows: First, the CI fragment samples were rinsed three times with distilled water to remove the unattached bacteria (i.e., planktonic cells), and subsequently, the attached cells were scraped from the surfaces using 250 µL of MH-Glu and cell scrapers (Greiner Bio-one). Then, 200 µL of the 250 µL used for scraping the cells was transferred into the first line of a 96-well plate (Greiner Bio-One), while the rest of the lines were filled with 180 µL of MH-Glu. Serial dilutions were carried out, and the cells were spotted onto either blood agar plates, which were then incubated at 37 °C under low oxygen for 20 h (*S. pneumoniae*) or Lysogenic Broth (LB, Difco) agar plates (*S. aureus*) incubated at 37 °C. Cell growth was monitored and determined by a viable cell count.

Biocompatibility—Human Dermal Fibroblasts: Studies on surgical waste material was approved by the Uppsala Ethical Review Board (no. 99398, 22/9 1999, cont., 2003). Written information was given to the patient and verbal informed consent was obtained. This procedure was chosen to reduce the stress on the patient and was approved by the ethical review board. No notes were made in the journal to reduce tracability and maintain patient confidentiality. Part of the auditory canal is routinely discarded during skull base surgery; this material was collected and the primary HF was isolated. Tissue was first placed overnight in dispase (Roche, Stockholm, Sweden) at 4 °C. The dermis was then isolated under a dissection microscope and placed in trypsin/EDTA (Sigma-Aldrich, Seelze, Germany) for 20 min followed by mechanical dissociation through vortexing. The trypsin reaction was stopped using culture media containing high glucose DMEM (Life Technologies) supplemented with 10% fetal bovine serum (FBS, Life Technologies) and 0.04% gentamicin. Larger pieces of tissue were removed and the cell suspension centrifuged for 5 min at 244 g. The pellet was re-suspended in cell culture media and seeded on uncoated cell culture plastic and placed in a humidified incubator at 37 °C and 5% CO_2. Cells were used after the third or fourth passage.

To assess cell health, alamarBlue (Life Technologies), a resazurin-based reagent, was used. The cell permeable resazurin is reduced by metabolically active cells into the red-fluorescing compound resorufin. Metabolic activity is then measured as an increase in fluorescence. This reagent has previously been used as an indicator of cell health and to measure cytotoxicity.[32,33]

The HFs were used at passages 3 and 4 and were dissociated by a 5 min incubation with trypsin/EDTA, which was inactivated by addition of culture media; then cells were counted. Approximately 500 cells per well were seeded in a 96-well plate and allowed to attach overnight. On the following day, CI fragments were cut into equal sized pieces using a sterile 2 mm punch biopsy needle (Miltex, York, PA, USA). The media was then replaced by 100 µL of media containing 10% alamarBlue per well and a single 2 mm fragment of coated or uncoated CI was subsequently placed in each well. Each plate contained triplicate control wells without any CI fragment, uncoated CI fragment, and CI fragment coated with 0.08 wt% or 0.32 wt% of ZnO-MgF_2. Wells without cells containing only media with alamarBlue served as a blank. The plates were transferred to a Wallac 1420 Victor^2 Microplate Reader (Perkin Elmer, Waltham, MA, USA) set for 530 nm/590 nm (excitation/emission) to record the fluorescent signal from degraded resorufin at 24 and 48 h. The experiment was performed six times.

Biocompatibility—Spiral Ganglion Explants: Spiral ganglion tissue was isolated from two P9 mouse cochleae. Murine temporal bones were harvested as residual tissues from sacrificed animals, the use of animals and the subsequent harvesting of tissues were approved by the regional animal ethics review board in Uppsala (Dnr. C346/11). Spiral ganglion explants were cultured as previously described.[34] Briefly the heads were placed in cooled DMEM (Life Technologies), the brain removed, and the cochleae isolated. The cochleae were then opened and each modiolus, containing the spiral ganglion, were isolated and cut into two pieces. Matrigel (growth factor reduced Matrigel, BD Biosciences, San Jose, CA, USA) was then mixed 1:1 with Neurobasal media (Gibco) containing: B27 supplement (1×, Gibco), 2×10^{-3} M L-glutamine (Gibco), 0.04% gentamicin, 20 ng mL^{-1} brain-derived neurotrophic factor (BDNF; R&D Systems), 20 ng mL^{-1} NT-3 (R&D Systems), and 20 ng mL^{-1} glial-derived neurotrophic factor (GDNF; R&D Systems). Two separate 20 µL drops of the Matrigel/media mix was placed in a 35 mm petri dish. One explant was placed in each drop with a 1 × 1 mm piece of uncoated CI in one drop and a 1 × 1 mm piece of 0.08 wt% ZnO-MgF_2 coated CI in the other. The gels were allowed to set for 30 min before being covered with Neurobasal media.

After 8 d cultures were fixed for 30 min using fresh 4% paraformaldehyde dissolved in PBS, they were washed and the cells permeabilized by a 30 min incubation with 0.4% Triton-X 100. After washing, Tuj1 primary antibody was applied for 48 h (1:600 dilution, cat.nr. 04–1049, Millipore, Billerica, MA, USA). Then, cells were washed and the secondary antibody applied overnight (1:600 dilution, Alexa Fluor 488, A11008, Life Technologies). Samples were then washed and the nuclei stained with 4′,6-diamidino-2-phenylindole (DAPI, 1:3000, Life Technologies) for 4 h. Samples were visualized using an inverted three color (358, 461, and 555 nm) fluorescence microscope equipped (TE2000-E, Nikon, Tokyo, Japan) with a three laser confocal system (C1, Nikon).

Supporting Information

Supporting Information is available from the Wiley Online Library or from the author.

Acknowledgements

This study was supported by the European Community 7th Framework Program on Research, Technological Development, and Demonstration. Project acronym: NANOCI; grant agreement no: 281 056. The work was also supported by ALF grants from Uppsala University Hospital and Uppsala University and the Tysta Skolan Foundation, Swedish Deafness Foundation (HRF).

Received: October 22, 2015
Revised: January 14, 2016
Published online: March 3, 2016

[1] T. Stöver, T. Lenarz, *Head Neck Surg.* **2009**, *8*, 1865.
[2] L. G. Rubin, B. Papsin, *Pediatrics* **2010**, *126*, 381.

[3] M. Ribeiro, F. J. Monteiro, M. P. Ferraz, *Biomatter* **2015**, *2*, 176.
[4] D. Teterycz, T. Ferry, D. Le, R. Stern, M. Assal, P. Hoffmeyer, L. Bernard, I. Uckay, *Int. J. Infect. Dis.* **2010**, *14*, 913.
[5] L. Zhang, D. Pornpattananangkul, C.-M. J. Hu, C.-M. Huang, *Curr. Med. Chem.* **2010**, *17*, 585.
[6] M. J. Hajipour, K. M. Fromm, A. A. Ashkarran, D. J. De Aberasturi, I. R. de Larramendi, T. Rojo, V. Serpooshan, W. J. Parak, M. Mahmoudi, *Trends Biotechnol.* **2012**, *10*, 499.
[7] H. Wang, M. Cheng, J. Hu, C. Wang, S. Xu, C. C. Han, *ACS Appl. Mater. Interfaces* **2013**, *5*, 11014.
[8] G. Paasche, L. Bögel, M. Leinung, T. Lenarz, T. Stöver, *Hearing Res.* **2006**, *212*, 74.
[9] A. Herman, A. P. Herman, *J. Nanosci. Nanotechnol.* **2014**, *14*, 946.
[10] E. Navarro, F. Piccapietra, B. Wagner, F. Marconi, R. Kaegi, N. Odzak, L. Sigg, R. Behra, *Sci. Technol.* **2008**, *42*, 8959.
[11] C. N. Lok, C. M. Ho, R. Chen, Q. Y. He, Y. Yu, W. Y. Sun, H. Tam, J. F. Chiu, C. M. Che, *J. Proteome Res.* **2006**, *5*, 916.
[12] J. F. Hernández-Sierra, F. Ruiz, D. C. C. Pena, F. Martínez-Gutiérrez, A. E. Martínez, A. D. J. P. Guillén, H. Tapia-Pérez, G. M Castañón, *Nanomedicine* **2008**, *4*, 237
[13] N. Jones, B. Ray, K. T. Ranjit, A. C. Manna, *FEMS Microbiol. Lett.* **2008**, *279*, 71.
[14] V. Thati, A. S. Roy, M. V. N. A. Prasad, C. T. Shivannavar, S. M. Gaddad, *J. Biosci. Tech.* **2010**, *1*, 64.
[15] J. T. Seil, T. J. Webster, *Acta Biomater.* **2011**, *7*, 2579.
[16] K. R. Raghupathi, R. T. Koodali, A. C. Manna, *Langmuir* **2011**, *27*, 4020.
[17] M. Ramani, S. Ponnusamy, C. Muthamizhchelvan, *Mater. Sci. Eng. C* **2012**, *32*, 2381.
[18] S. Paul, D. K. Ban, *Int. J. Adv. Chem. Eng. Biol. Sci.* **2014**, *1*, 1507.
[19] O. A. Al-Hartomy, M. Mujahid, *Am. J. Biol. Chem.* **2014**, *2*, 17.
[20] A. Gedanken, *Ultrason. Sonochem.* **2007**, *14*, 418.
[21] A. Gedanken, N. Perkas, in *Surface Coatings* (Eds: M. Rizzo, G. Bruno), Nova Science Pub,New York, USA **2009**, Ch. 9.
[22] G. Applerot, J. Lellouche, N. Perkas, Y. Nitzan, A. Gedanken, E. Banin, *RSC Adv.* **2012**, *2*, 2314.
[23] J. Lellouche, A. Friedman, R. Lahmi, A. Gedanken, E. Banin, *Int. J. Nanomed.* **2012**, *7*, 1175.
[24] J. Lellouche, A. Friedman, J. P. Lellouche, A. Gedanken, E. Banin, *Nanomedicine.* **2012**, *8*, 702.
[25] A. Homsy, E. Laux, J. Brossard, H. Whitlow, M. Roccio, S. Hahnewald, P. Senn, P. Mistrik, R. Hessler, T. Melchionna, C. Frick, H. Lowenheim, M. Muller, U. Wank, K. Wiesmuller, H. Keppner, *Hearing Balance Commun.* **2015**, *4*, 153
[26] N. Perkas, G. Amirian, G. Applerot, E. Efendiev, Y. Kaganovskii, A. V. Ghule, B.-J. Chen, Y. C. Ling, A. Gedanken, *Nanotechnology* **2008**, *19*, 435604.
[27] I. Perelshtein, G. Applerot, N. Perkas, J. Grinblat, E. Hulla, E. Wehrschuetz-Sigl, A. Hasmann, G. Guebitz, A. Gedanken, *ACS Appl. Mater. Interfaces* **2010**, *2*, 1999.
[28] M. Chen, Y. Qingsong, S. Hongmin, *Int. J. Mol. Sci.* **2013**, *14*, 18488.
[29] D. Roe, B. Karandikar, N. Bonn-Savage, B. Gibbins, J. B. Roullet, *J. Antimicrob. Chemother.* **2008**, *61*, 869.
[30] A. Epstein, T. Wong, R. Belisle, E. Boggs, J. Aizenberg, *Proc. Natl. Acad. Sci. U.S.A.* **2012**, *109*, 13182.
[31] O. Yamamoto, *Int. J. Inorg. Mater.* **2001**, *3*, 643.
[32] R. Hamid, Y. Rotshteyn, L. Rabadi, R. Parikh, P. Bullock, *Toxicol. In Vitro* **2004**, *18*, 703.
[33] G. R. Nakayama, M. C. Caton, M. P. Nova, Z. Parandoosh, *J. Immunol. Methods* **1997**, *204*, 205.
[34] F. Edin, W. Liu, H. Li, F. Atturo, P. U. Magnusson, H. Rask-Andersen, *Acta Otolaryngologica* **2014**, *134*, 1211.